TRANSITION CONTROL ON A TRANSONIC LAMINAR AIRFOIL WITH SUCTION PANEL

L. Jørgensen, W. Nitsche

Institut für Luft- und Raumfahrt, Technische Universität Berlin, F. R. G.
Marchstr. 14, D-10587 Berlin

Abstract

The efficiency of future airliners can be improved significantly by applying laminar wing technology. Hybrid laminar flow-control designs employ suction panels at the wing leading edge to stabilize the laminar b.l. The present investigation was aimed at a control system for such suction panels. For this purpose, a transonic laminar airfoil with a segmented suction panel was used to develop a sensor based monitoring system. The system measures on-line the transition position on the active suction panel without disturbing the laminar flow. Tests were performed at different flow and b.l. suction conditions and checked against reference techniques. Furthermore, the sensor system was employed to control the suction distribution of the airfoil in order to minimize the total drag.

Nomenclature

A	van Driest damping constant
c	chord length
c_f	skin friction coefficient
c_q	suction coefficent
c_w	airfoil drag coefficient
K1	constant
M	Mach-number
p	pressure
pdf	probability density function
Re	Reynolds number
Tu	turbulence intensity
U	voltage
x,y,z	coordinates
x_t	transition location
α	attack angle
σ	standard deviation
κ	von Karman constant

Indices

∞	free-stream conditions
+	non-dimensional values
RMS	root mean square

Introduction

The laminar wing technology promises a significant reduction in aircraft drag and thereby in fuel consumption and operating costs [1]. On conventional wings the transition from a laminar b.l. state (with low skin friction) to turbulent b.l. (with significantly higher skin friction) occurs near the leading edge (Fig. 1a). On a laminar wing the transition is delayed until further downstream, causing a reduction in friction drag. For smaller aircraft, a laminar wing may be achieved already by means of a suitable airfoil design and including a good surface quality. This design approach is called natural laminar flow technology (NLF, Fig. 1b) and is applied to general aviation aircraft and regional airliners.

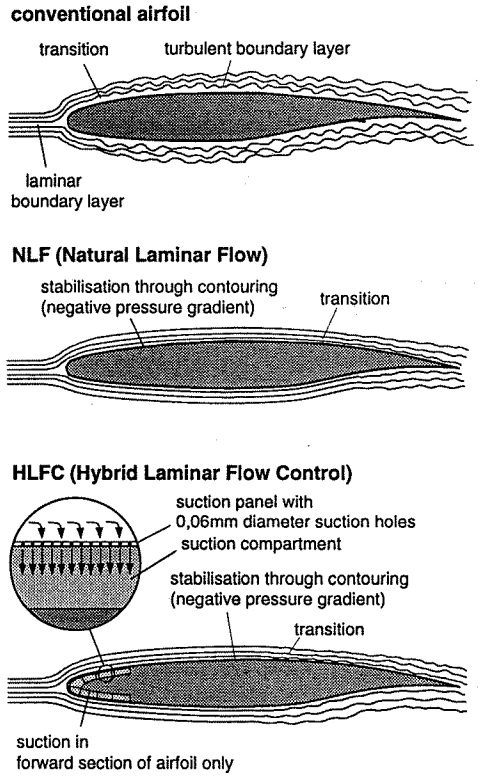

Fig. 1 Conventional airfoil and application of laminarization techniques

Larger aircraft, however, require active b.l. stabilization due to their higher cruise Reynolds number and wing sweep. Attachment line and cross-flow instabilities cause premature transition at the leading edge and the forward region of the wing. The hybrid laminar flow concept (HLFC, Fig. 1c) applies b.l. suction with porous suction panels at the leading edge in combination with a suitable airfoil contour downstream. A typical b.l. suction system consists of skin panels with very small suction holes (≈60µm diameter). A small amount of air is sucked through the holes into the suction compartment. This stabilizes the boundary layer and delays transition.

The suction compartment is subdivided into separate chambers. As the external pressure variies in chordwise direction corresponding to the pressure distribution, the suction level has to be adjusted accordingly. As the power required for the suction system curtails the obtained drag reduction, it is necessary to optimize the suction rate and distribution. To opperate a control system for the suction system, the transition location on the wing as well as on the suction panel must be known. Different measuring techniques have been developed and used in recent laminar research, but not all are suitable for applications in a future control systems. The ideal system should deliver a real-time information about the b.l. state covering most of the wing surface including the active suction panel, without disturbing the laminar boundary layer.

The hot-film technique uses thin, electrically heated metal films on a plastic carrier film, which are placed on the wing surface [2]. The convective heat transfer can be related to the local wall shear stress, the dynamic part of the signal can be used to state the flow condition (laminar/transitional/turbulent). Hot-films may be arranged in sensor arrays, resulting in a sensor system with good spatial and temporal resolution. Drawbacks are the vulnerability of the sensors and blockade effects when using hot film arrays.

Another technique using the analogy between heat transfer and wall shear stress is infrared thermography [3]. An infrared camera gives a picture of the wing surface temperature, where laminar areas have different temperatures than turbulent ones due to differences in heat transfer. While giving good results in NLF experiments a use on the metallic suction panel is not possible. To check all laminarized surfaces would require complicated camera installations.

A very promising technique is the use of small microphones to detect dynamic pressure fluctuations in the boundary layer [4][5]. Placing the microphone under small pressure port or the porous suction surface gives a good protection of microphone membrane while trading in some sensitivity. The present paper shows the application of microphones to detect the transition location on a laminar airfoil with b.l. suction. It is shown how the sensor signals can be used to optimize the suction distribution.

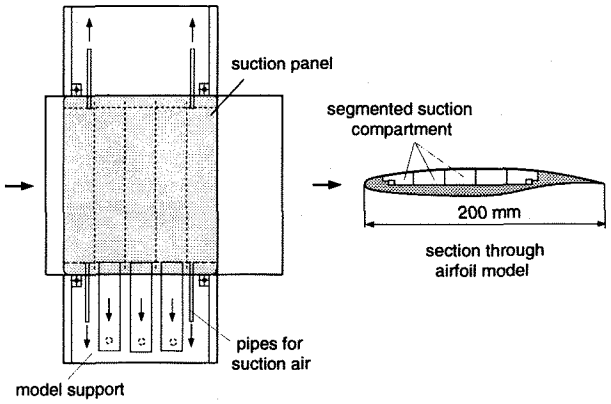

Fig. 2 LV2 airfoil model with segmented suction panel

Experimental apparatus

After pretests on a low speed airfoil [6] a 2-D airfoil model for testing in the ILR transonic wind tunnel was build as shown in Fig. 2. The model used a DLR-LV2 section, a laminar wing airfoil developed for a regional airliner [7][8]. The model has a chord length of 200mm, featuring a perforated suction panel from x/c=0.05 to 0.75. The suction panel consisted of a 0.8mm thick stainless steel sheet with 60µm diameter suction holes at 0.6mm spacing. The suction holes were drilled by electron beam, the panel used for the experiments was supplied from DASA-Airbus. The suction chamber under the panel was subdivided into separate compartments, allowing a streamwise variation of the suction rate.

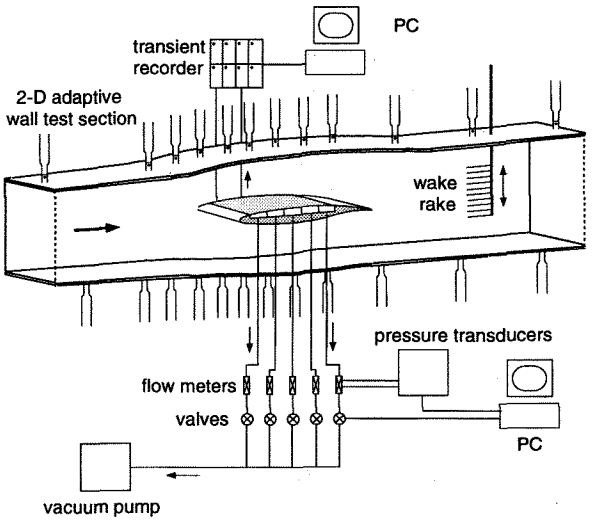

Fig. 3 Test set-up in the transonic wind tunnel

The tests were performed in the transonic wind tunnel of the ILR (Fig. 3). The wind tunnel is driven by an radial compressor connected to a 400kW DC electric

motor. The tunnel can be operated continously. The freestream turbulence of the tunnel is between 0.2% and 0.3%, depending on the operating Mach-number.

The 2D-adaptive-wall test section of the ILR transonic tunnel with a cross section of 150x150mm was used for the tests. The upper and lower wall can be contoured to minimize wind tunnel wall interferences. The wind tunnel is equipped with an automatic pressure measurement system (PSI 780B) with 224 channels and a Laser-2-Focus anemometer.

The suction for the panel was provided by a powerful vacuum pump. The mass flows and thereby the suction rates in the individual compartments were measured by five venturi-flowmeters. The pressures of the venturis were recorded by the wind-tunnel pressure measurement system, transfered to a PC and the actual suction rate was calculated on-line. An equivalent drag coefficient resulting from the suction system power requirement was calculated to compare with the achieved drag reduction, assuming an efficency factor of 0.85 for the suction system. The flow rate was adjusted by individual servo valves, controlled by a PC.

To quantify the amount of the accomplished drag reduction the airfoil drag was measured with a traversing wake rake. The rake was mounted one chord length downstream of the airfoil, traversing of the rake and pressure measurement was computer-controlled and the airfoil drag was calculated and displayed on-line.

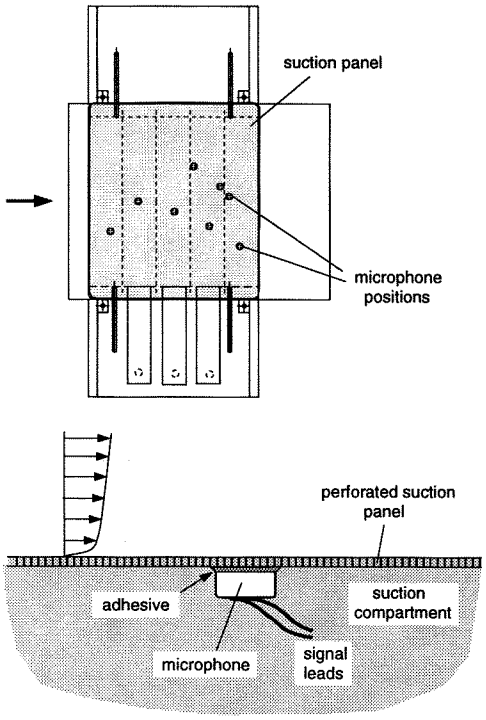

Fig. 4 Microphone positions and attachment under the suction panel

To control the transition location, a simple nonintrusive measuring system based on a microphone array was developed. Miniature microphones with a diameter of 6mm were used. Fig. 4 shows the sensor arrangement on the panel and the attachment under the panel. The microphones were placed inside of the individual suction compartments and glued to the suction panel. The dynamic pressures of the boundary layer are measured through the suction holes. In the transition region the highest pressure fluctions are present. The sensors were arranged as an array. A more detailled description of the test set-up is given in [9].

Sensor system development

After prelimenary tests the sensors were placed under the suction panel. It was found that the transition position could easily be detected from monitoring the time traces of the microphones. Fig. 5 shows the time traces of selected sensors at different Mach-numbers and with and without b.l. suction.

The top row shows sensor signals at a free-stream Mach-number of 0.30 without b.l. suction. The second sensor shows the highest signal power, indicating the transition location. Turbulent spots may be seen in the trace of the first sensor, lying upstream of the transition. The second row shows the signals after b.l. suction was applied. A uniform suction rate for all compartments was used. The transition position is now delayed and can be seen at the fifth sensor.

As the free-stream Mach-number is increased to 0.40 the transition for the case without b.l. suction moves upstream to the first sensor. Application of b.l. suction now moves the transition downstream to the third sensor. The general signal level is increased when compared to the signals at M_∞=0.30.

The two bottom rows shows the sensor signal for a free-stream Mach number of 0.60. Without suction the transition is at the first sensor and moves to the second sensor as suction is applied. The signal level is further increased, resulting in overranging of the sensors in the transition region, but the transition is still clearly detectable as the background noise remains low.

Fig. 6 shows frequency spectra corresponding to the time traces shown in Fig. 5. The level of the spectra reflects the power of the time traces. The sensors in the transition region show a higher amplitude level than the sensors in laminar and turbulent regions. In some cases the spectra of laminar and turbulent sensors show diffences in slope. The turbulent spectrum has a higher level in higher frequencies in comparision to lower frequencies than the laminar spectrum.

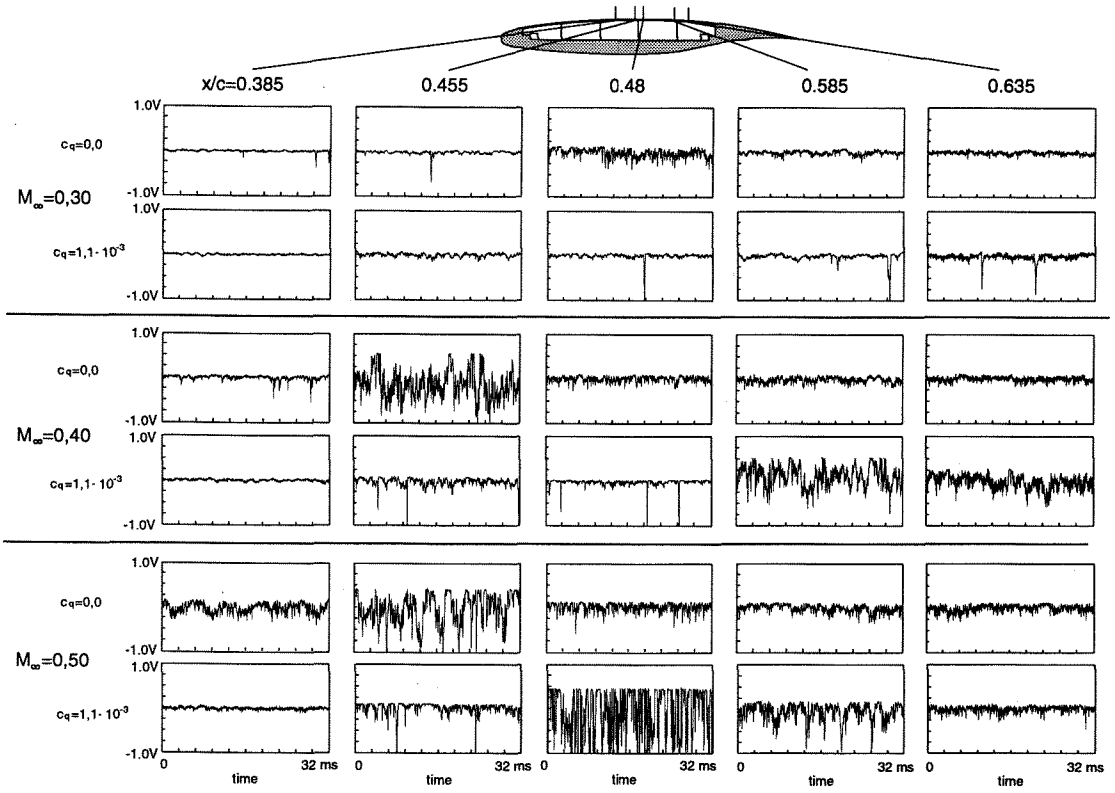

Fig. 5 Time traces of selected microphones for different Mach-numbers and suction distributions, α=0,0°

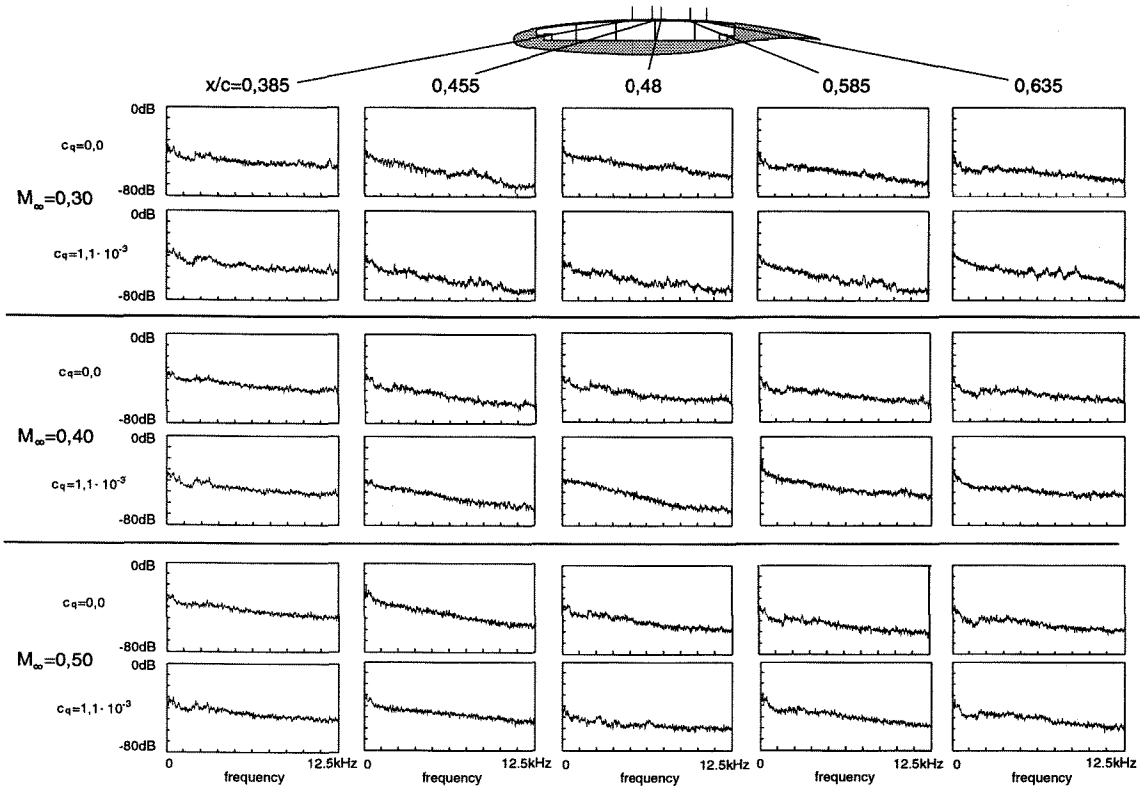

Fig. 6 Frequency spectra of selected microphones for different Mach-numbers and suction distributions, α=0,0°

Fig. 6 shows frequency spectra corresponding to the time traces shown in Fig. 5. The level of the spectra reflects the power of the time traces, the sensors in the transition region show a higher amplitude level than the sensors in laminar and turbulent regions. In some cases the spectra of laminar and turbulent sensors show diffences in their slope. The turbulent signal has a higher level of higher frequencies in comparision to lower frequencies than the laminar signal.

Fig. 7 shows statistical analysis of the time traces of Fig. 5 for a free-stream Mach number of 0.40 with b.l. suction applied. The probability density functions (pdf) for each time trace are shown, compared to the Gaussian normal distribution (dotted line). The time traces upstream of the transition region show single spikes caused by turbulent spots. This results in an asymmetrical, peaky pdf. The sensors in the transition region, where the b.l. state changes between laminar and turbulent, show a broader pdf.

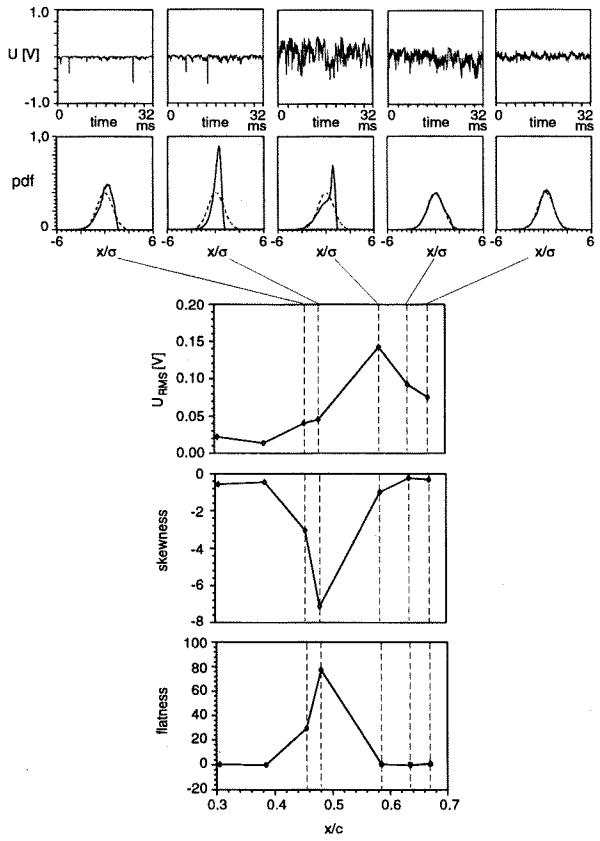

Fig. 7 Statistical values and probability density functions, M_∞=0.40, α=0.0°

The form of the pdf can be characterised by the skewness and flatness. These values are drawn up in the lower part of Fig. 7 in comparision with the RMS value. The sensor directly upstream of the transition displays a maximum in the flatness and a minimum in the skewness.

After performing the tests with the microphone array, reference measurements were undertaken with the CPM3-method and Laser-2-Focus velocimeter.

The Computational Preston-tube Method (CPM3) is a wall shear stress measurement technique [10], based on the Preston-tube method. A probe with three different sized Preston tubes is used to measure the total pressure at three different levels of the boundary layer. The velocity profile of the boundary layer is calculated to match the three measured velocities by variation of the free parameter K_1 in the boundary layer law, based on an extended van-Driest law:

$$u_i^+ = \int_0^{y_i^+} \frac{2(1+p^+y^+)dy^+}{1+[1+4(K_1y^+)^2(1+p^+y^+)(1-exp(-y^+\sqrt{1+p^+y^+}/A^+))^2]^{0.5}}$$

$$u^+ = \frac{u}{u_\tau}$$

$$y^+ = \frac{yu_\tau}{\nu}$$

$$p^+ = \frac{\nu}{\rho u_\tau^3}\frac{dp}{dx}$$

This law of the wall correlates the dimensionless velocity u^+ with the wall distance parameter y^+ and includes the pressure gradient p^+ build with the local pressure gradient. A^+ is the van-Driest damping constant (A^+=26) whereas the iteration parameter K_1 replaces the von Karman constant (κ=0.4)[11].

Fig. 8 shows the probe as used on the transonic laminar airfoil. To take the static pressure at the probes chordwise location a tube was attached to the bottom of the suction panel, measuring the static pressure through the panel suction holes.

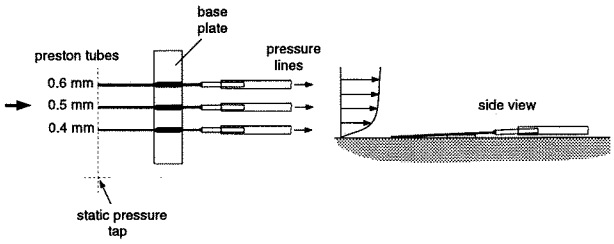

Fig. 8 CPM3-probe for wall shear stress measurements

The CPM3-probe was placed at different positions on the profile and the local Reynolds-number was varied by changing the free-stream Mach-number. The pressures were recorded and the local wall shear stress and drag coefficent were calculated. The measurements were performed at the same flow conditions with and without b.l. suction. The results are shown in Fig. 9 and Fig. 10. The measured skin friction coefficents are drawn up in comparison to the values for the flat plate with laminar (Blasius) and turbulent (Schulz-Grunow) boundary layer.

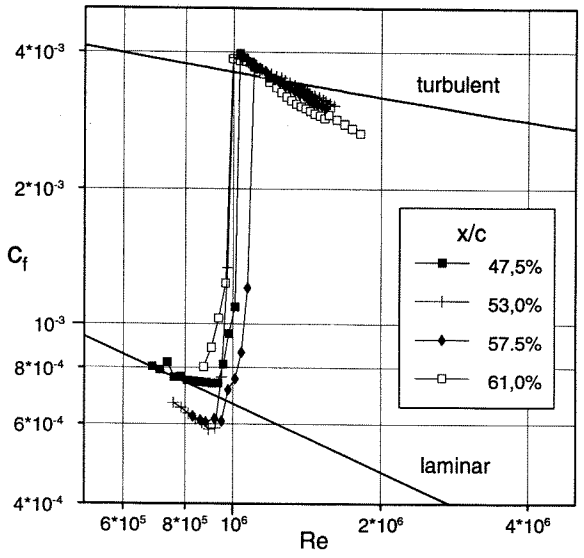

Fig. 9 Skin friction measurements without b.l. suction

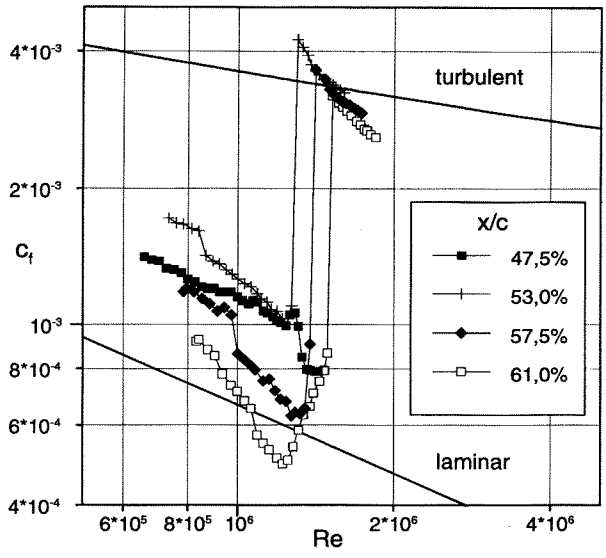

Fig. 10 Skin friction measurements with b.l. suction activated (c_q=0.6·10^{-3})

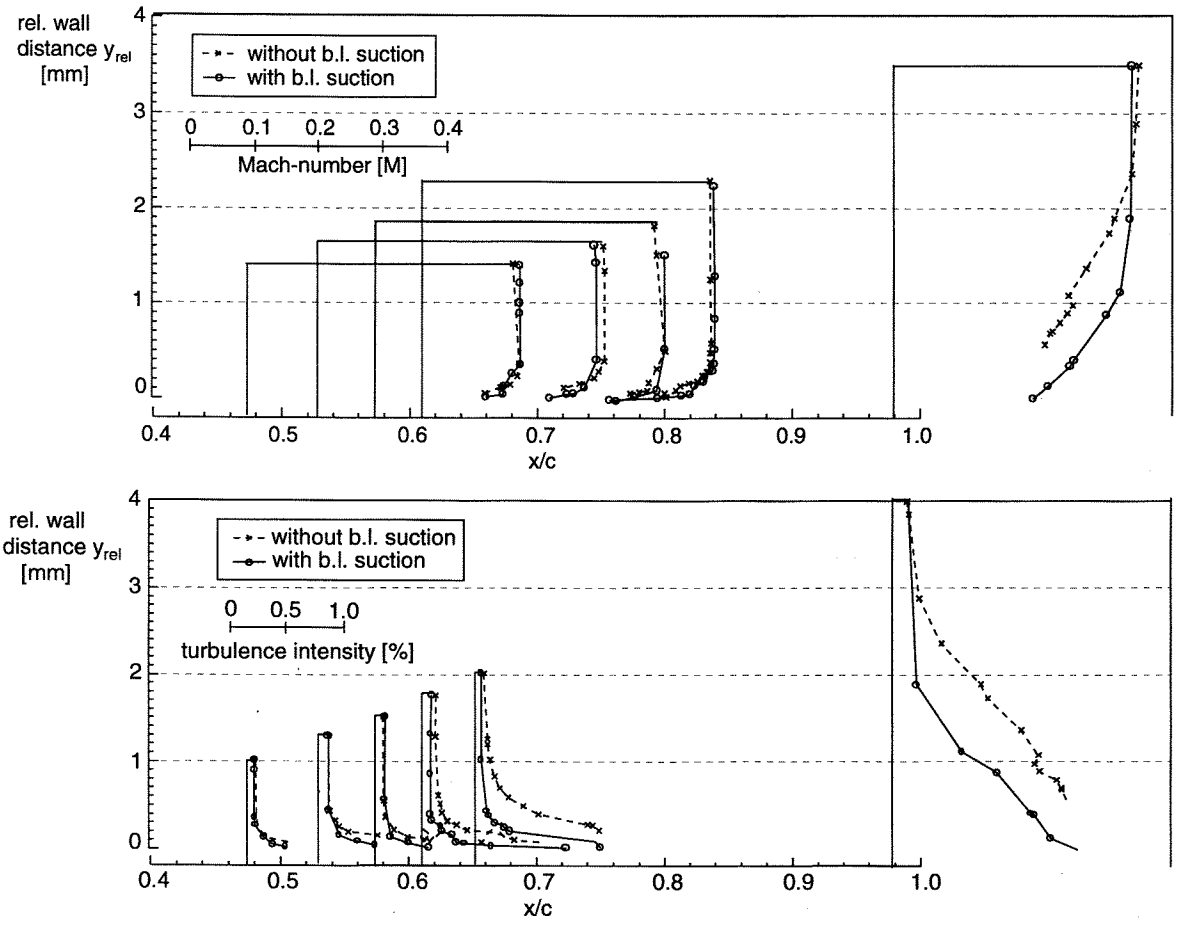

Fig. 11 Velocity profiles as measured with Laser-2-Focus anemometer, M_∞=0.35

The transition from a low friction coefficent to a higher lever characterises the transition location. As can clearly be seen, the transition moves to higher Reynolds-numbers as the b.l. suction is activated. Furthermore, it can be seen that the laminar skin friction is increased in case of b.l. suction.

The transition from a low friction coefficent to a higher lever characterises the transition location. As can clearly be seen, the transition moves to higher Reynolds-numbers as the b.l. suction is activated. Furthermore, it can be seen that the laminar skin friction is increased in case of b.l. suction.

Further reference measurements were carried out using a Laser-2-Focus anemometer. It was used to measure boundary layer profiles and turbulence intensities for flow cases with and without b.l. suction, as shown in Fig. 11.

In the top graph of the figure the velocity profiles of the two flow cases are compared. The boundary layer with suction activated is thinner than in the case without suction due to the stabilizing effect of the b.l. suction. This can be seen very cleary at the last measurement position.

The Laser-2-Focus anemometer calculates a turbulence intensity from the measured velocity distribution. This value is higher than the actual turbulence level of the flow, but it may be used as a qualitative indicator for the flow turbulence. The bottom chart in Fig. 11 shows the turbulence intensity profiles corresponding to the velocity profiles. The profiles for the case without suction show significantly higher turbulence intensities than the stabilized boundary layer with suction.

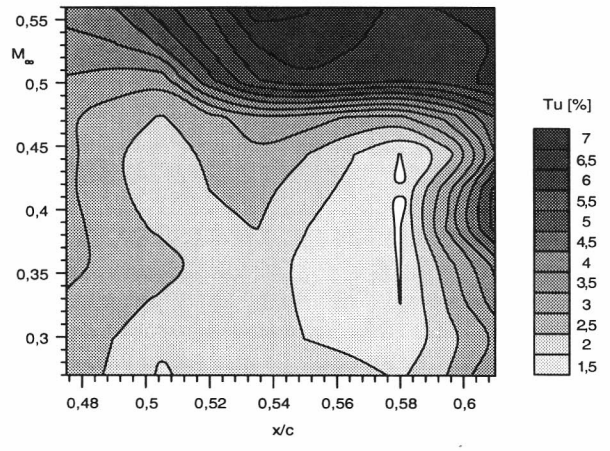

Fig. 12 Turbulence intensities as measured in the boundary layer, wall distance 1.0mm, without suction

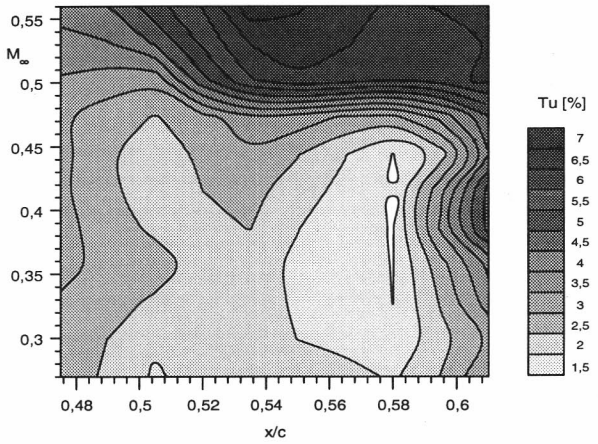

Fig. 13 Turbulence intensities as measured in the boundary layer, wall distance 1.0mm, boundary layer suction activated (c_q=0.6 10^{-3}).

Further laser measurements were made to detect the transition location on the panel. The measuring volume of the laser velocimeter was placed at a distance of 0.1 mm normal to the wall at several chordwise stations to measure the local turbulence intensity. An increase in the turbulence level marks the transition. The measurements were performed at the same flow conditions as with the other techniques at an angle of attack of α=0.0° and with variing freestream Mach-numbers. The results from the turbulence intensity measurements without and with b.l. suction are shown in Fig. 12 and Fig. 13. A significant streamwise delay of transition can be seen as b.l. suction is applied.

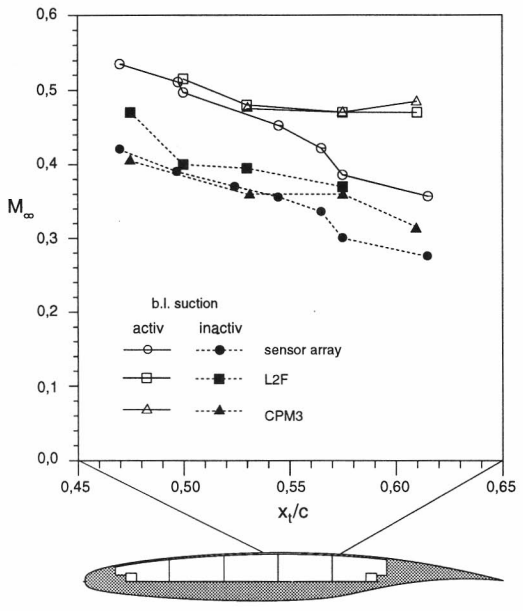

Fig. 14 Comparision of the different measuring techniques

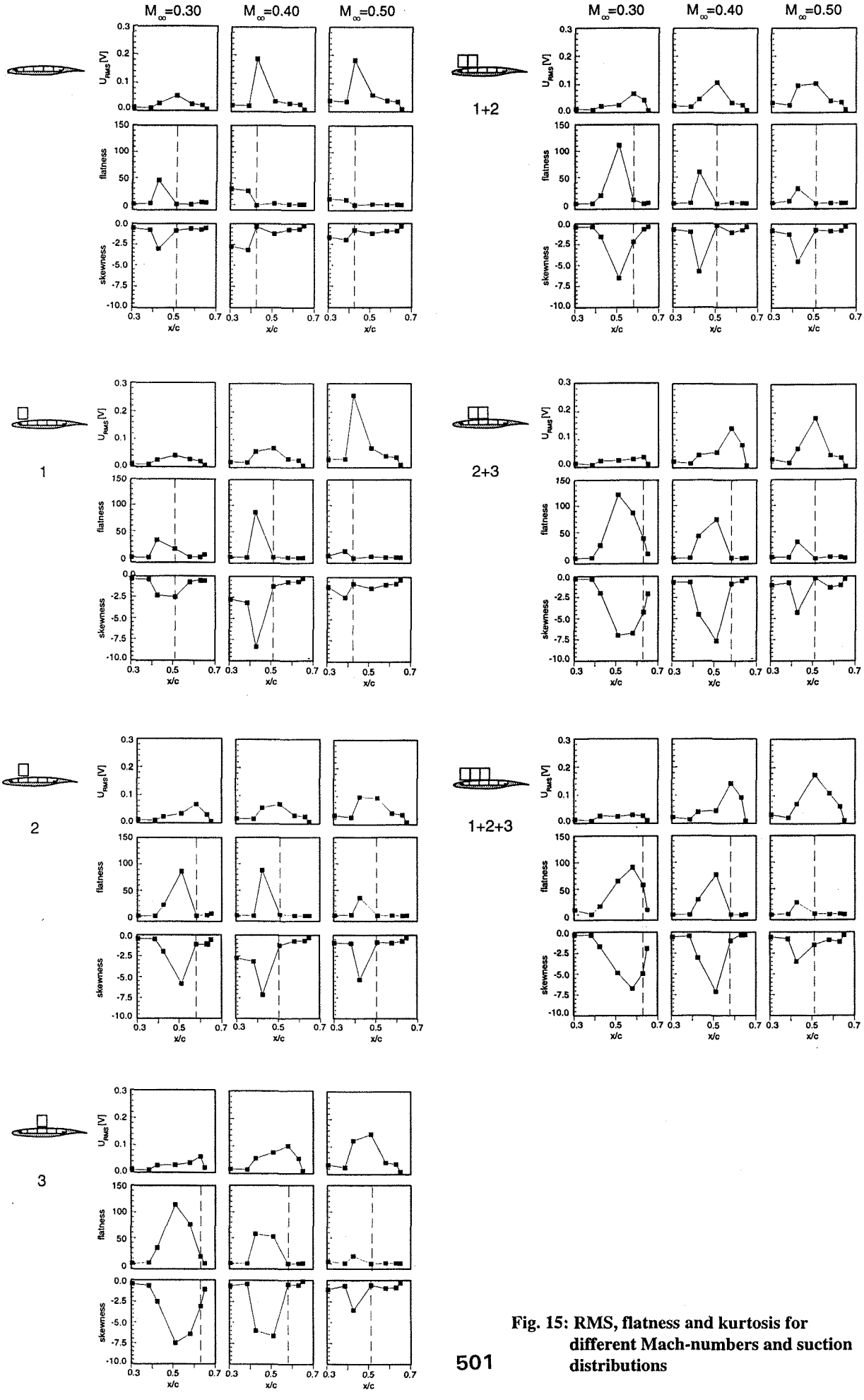

Fig. 15: RMS, flatness and kurtosis for different Mach-numbers and suction distributions

A comparision of the different measuring techniques is shown in Fig. 14. All techniques show significant transition delay by appling b.l. suction. The agreement is good, taking into consideration that the model was taken from the tunnel und rearranged several times to get the measurements.

Suction rate optimization

After developing the sensor system and testing it in comparision with different measuring techniques variations in suction distributions were undertaken. Fig. 15 shows a compilation of tests at different Mach-numbers and suction distributions. Beginning with the reference case without suction the results for three Mach-numbers (0.30, 0.40, 0.50) are shown. In the next tests single suction compartments were activated, followed by combinations of suction compartments. It is in each case possible to determine the transition location from the RMS peak value within a certain accuray as the microphones have a minimal distance due to the models small size.

Also shown in Fig. 15 are the statistical values (skewness and flatness) for the same tests. The traces show marked minima in case of the skewness and maxima for the flatness. These peak values are generaly one sensor position upstream of the corresponding RMS maxima, as they are caused by the turbulent spots ahead of the transition. The results show that the statistical values may be used to get additional transition criteria.

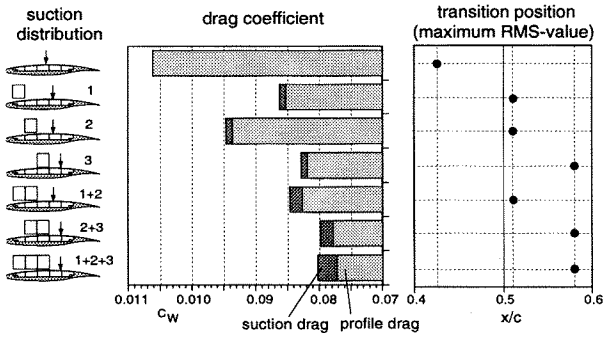

Fig. 16 Suction rate variation: drag measurement and transition location as detected by sensor array, M_∞=0.40, α=0.0°

Fig 16 gives an example of how the sensor system may be used to optimize the suction distribution. The figure shows the transition location as measured with the sensor system and the airfoil drag for different suction distributions as shown in Fig. 15. The total drag is composed by the airfoil drag as measured by the wake and the suction drag due to the suction power required.

The top row shows the result for the refence case without b.l. suction. The next rows show the values as the first three compartments are activated separately. Here, the third compartment gives the highest drag reduction. The other rows show suction cases with combinations of compartments. The case were all compartments are used has the least profile drag, but when adding the suction drag the total drag is slightly higher than the combination of the second and third compartment.

To optimize the total drag in a future full-scale application one would start the process by applying maximum suction and measuring the transition location. The suction rate could now be decreased, as long as the transition position remains the same and does not travel upstream.

Determination of b.l. state

In the previous chapter it was shown how the sensor system could be used to optimize the suction distribution by detecting the transition location. Preferably the system should also be able to determine the b.l. state in case the transition is not situated on the array. Such a case exists if the transition is caused by leading edge contamination.

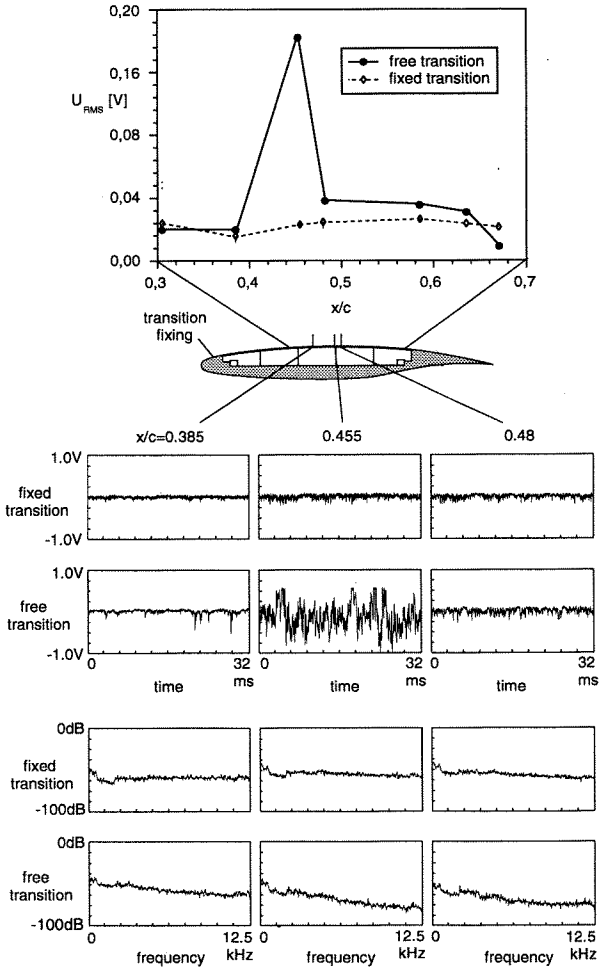

Fig. 17 Comparison of flow with fixed transition (x/c=0.05) with free transition, M_∞=0.40, α=0.0

To simulate this flow case, the transition was fixed on the upper side of the airfoil at x/c=0.05. Fig. 17 compiles results for measurements with fixed transition in comparison with measurements at the same flow condition at free transition. While the time traces in case of a fixed transition show very similar amplitudes, the traces in case of fixed transition show very different amplitudes. This is reflected in the RMS-values, staying on an equal level in case of fixed transition and showing a marked maximum in the case of free transition.

The frequency spectra are very similar for fixed transition, showing a relativly high level of higher frequencies typical for turbulent b.l. In comparison the frequency spectrum for the laminar b.l. has a lower level.

A system for determing the b.l. state could utilise these characteristics by evaluating the frequency spectra of the measured signals.

Conclusion

The present investigation was aimed on a control system for suction panels on hybid laminar wings. For this purpose, a sensor system was developed to measure the transition location on an active b.l. suction panel. The tests were performed on a transonic airfoil model with a segmented suction panel. The sensor microphones were mounted on the inner side of the panel to measure the pressure fluctuations of the boundary layer through the suction holes. Tests were conducted at different free-stream Mach-numbers and suction distributions. The transition position is marked by a peak in the RMS-value of the sensor array. Additional detection methods using statistical values were shown. The obtained results were verified with reference measurements performed with Preston tubes and a Laser-2-Focus velocimeter.

Furthermore, the system was used to demonstate how the suction distribution may be optimized in order to minimize the drag. A variation of suction distributions were tested and the actual transition location was derived from the sensor array. In this way it was possible to control the suction distribution to get the minimal total drag, i.e. to achieve the minimal aerodynamic drag with the least suction power needed.

Further experiments will aim on tests on a swept wing model. The use of a swept wing model will enable the studies of cross-flow instabilities which are dominant on large-scale airliner wings.

Acknowledgements

The authors are grateful for the Geman Science Foundation (DFG) for financial support and for DASA-Airbus for the supply of suction panels.

References

[1] J. P. Robert: Drag Reduction: An Industrial Challenge, AGARD-R-786-2 (1992)

[2] H.-P. Kreplin, G. Höhler: Application of the Surface Hot Film Technique to Laminar Flow Investigations, DGLR-Bericht 90-06 (1990)

[3] A. Quast: Detection of Transition by Infrared Image Technique, Pro. of the Int. Congress on Instrumentation in Aerospace Simulation Facilities, 1987

[4] J. Rickards, R. V. Barett: Development of an Acoustic Detector with Application to Boundary Layer Control by Suction, DGLR-Bericht 92-06-046 (1992)

[5] R. Barett, W. Kühn: Anwendung eines traversierbaren Mikrophonarrays zur Untersuchung einer gestörten laminaren Grenzschicht an abgesaugten feinperforierten Blechen, ILR-Mitt. 295 (1995) pp.147-155

[6] L. Jørgensen, W. Nitsche: Untersuchungen zu einem sensorischen Überwachungssystem für Absaug-Panel an Hybrid-Laminarflügeln. ILR-Mitteilung 289 (Berlin 1994)

[7] G. Redecker, K. H. Horstmann, H. Köster, A. Quast: Investigations on High Reynolds Number Laminar Airfoils, ICAS-86-1.1.3 (1986)

[8] G. Redecker, R. Müller, A. Blanchard, J. Reneaux: Evaluation of Transonic Laminar Airfoil under Cyrogenic Conditions Including Stability Analysis and Computational Results, DGLR-Bericht 92-06-019 (1992)

[9] L. Jørgensen: Sensorgestützte Steuerung der Grenzschichtabsaugung an einem transsonischen Laminarprofil, PhD thesis TU Berlin 1996, to be published

[10] W. Nitsche: A Computational Preston tube Method, Turbulent Shear Flows 4, Berlin/Heidelberg: Springer-Verlag 1985

[11] W. Nitsche: Strömungsmeßtechnik, Springer-Verlag Berlin Heidelberg 1994